



Published in final edited form as:

Nat Commun. ; 5: 5411. doi:10.1038/ncomms6411.

Unencapsulated *Streptococcus pneumoniae* from conjunctivitis encode variant traits and belong to a distinct phylogenetic cluster

Michael D. Valentino^{1,2,3}, Abigail Manson McGuire³, Jason W. Rosch⁴, Paulo J. M. Bispo^{1,2}, Corinna Burnham⁴, Christine M. Sanfilippo^{5,†}, Robert A. Carter⁴, Michael E. Zegans⁶, Bernard Beall⁷, Ashlee M. Ear³, Elaine I. Tuomanen⁴, Timothy W. Morris^{5,‡}, Wolfgang Haas^{1,2}, and Michael S. Gilmore^{1,2,3,*}

¹Department of Ophthalmology, Massachusetts Eye and Ear Infirmary, 243 Charles St. C703, Boston, MA 02114, USA

²Department of Microbiology and Immunobiology, Harvard Medical School, 77 Ave Louis Pasteur, Boston, MA 02115, USA

³The Broad Institute of MIT and Harvard, 320 Charles St. Cambridge, MA 02141, USA

⁴Department of Infectious Diseases, St. Jude Children's Research Hospital, 262 Danny Thomas Pl., Memphis, TN 38105, USA

⁵Bausch and Lomb, Inc., 1400 Goodman St. N., Rochester, NY 14609, USA

⁶Department of Microbiology and Immunology, Geisel School of Medicine at Dartmouth, 1 Rope Ferry Rd., Hanover, NH 03755, USA

⁷Streptococcus Laboratory, Centers for Disease Control and Prevention, 1600 Clifton Rd., Atlanta, GA 30333, USA

Abstract

Streptococcus pneumoniae, an inhabitant of the upper respiratory mucosa, causes respiratory and invasive infections as well as conjunctivitis. Strains that lack the capsule, a main virulence factor and the target of current vaccines, are often isolated from conjunctivitis cases. Here we perform a comparative genomic analysis of 271 strains of conjunctivitis-causing *S. pneumoniae* from 72

Users may view, print, copy, and download text and data-mine the content in such documents, for the purposes of academic research, subject always to the full Conditions of use:http://www.nature.com/authors/editorial_policies/license.html#terms

*To whom correspondence should be addressed: Massachusetts Eye and Ear Infirmary, 243 Charles Street, 7th Floor, Connector Building, Boston, MA 02114. Phone: (617) 573-3845. Fax: (617) 573-4290. michael_gilmore@meei.harvard.edu.

†Present address: Upstate Stem Cell cGMP Facility, University of Rochester, 601 Elmwood Ave., Rochester, NY, 14642, USA

‡Present address: Actelion Clinical Research, 1820 Chapel Ave., Cherry Hill, NJ, 08002, USA

Author's contributions. MSG and MDV conceived and designed the study. MDV, AMM, PJMB, CB, CMS, RAC performed the experiments. MDV, AMM, JWR, MSG contributed to the analysis and interpretation of the results. The manuscript was written by MDV and MSG. MEZ, BB, TWM, WH provided strains from conjunctivitis. AME, EIT provided additional guidance during manuscript preparation.

Accession codes. Draft genome sequences have been deposited in the DDBJ/EMBL/GenBank databases under BioProject PRJNA22902. See Supplementary Data 2 for individual accession codes for the draft genome sequences.

Supplementary Information accompanies this paper.

Competing financial interests: The authors declare no competing financial interests.

postal codes in the US. We find that the vast majority of conjunctivitis strains are members of a distinct cluster of closely related unencapsulated strains. These strains possess divergent forms of pneumococcal virulence factors (such as CbpA and neuraminidases) that are not shared with other unencapsulated nasopharyngeal *S. pneumoniae*. They also possess putative adhesins that have not been described in encapsulated pneumococci. These findings suggest that the unencapsulated strains capable of causing conjunctivitis utilize a pathogenesis strategy substantially different from that described for *S. pneumoniae* at other infection sites.

Keywords

Streptococcus pneumoniae; conjunctivitis; non-typeable; unencapsulated; comparative genomics

Introduction

Streptococcus pneumoniae is a leading cause of invasive infections including pneumonia, meningitis, and sepsis, as well as non-invasive infections including pharyngitis and otitis media. The polysaccharide capsule, a key virulence factor, is the target of current vaccines¹⁻³. Vaccination has substantially reduced morbidity and mortality³, but has had limited impact on conjunctivitis, infection of the mucous membrane covering the eye and lining the eyelids⁴.

We recently collected 271 *S. pneumoniae* isolates during the course of clinical trials for the treatment of bacterial conjunctivitis⁵⁻⁷, and found that over 90% were unencapsulated⁸, and hence unaffected by current vaccine design. Unencapsulated *S. pneumoniae* strains have caused large conjunctivitis outbreaks in schools and colleges⁹⁻¹³, military training facilities in the US¹⁴, and at other locations worldwide¹⁵. Recent outbreaks have involved one multilocus sequence type (MLST) in particular, ST448¹³. However, a previous study of epidemiologically unrelated conjunctivitis cases found that most cases were caused by encapsulated strains⁴. That study examined isolates prior to the widespread use of the PCV7 vaccine introduced in 2000⁴.

With a view toward assessing the impact of the vaccine and improved vaccine design, and to better understand the diversity of strains and genetic basis for *S. pneumoniae* pathogenesis in conjunctivitis, here we describe the results of an extensive comparative analysis of *S. pneumoniae* currently associated with conjunctivitis.

Results

Epidemiology of conjunctivitis

To determine the diversity of *S. pneumoniae* causing conjunctivitis, 271 strains⁵⁻⁸ were characterized by MLST¹⁶ (Fig. 1, Supplementary Data 1). Sequence type ST448^{17,18} was found to cause the majority of infections (67.2%). The next most common types caused substantially fewer: ST344 (8.9%), ST1186 (4.8%), ST2315 (4.4%). Together, 10 different sequence types of unencapsulated *S. pneumoniae* accounted for 90.8% of conjunctivitis cases. A diverse set of strains of *S. pneumoniae* from other types of infections, for which closed genomes are available in Genbank, were included for comparison (Supplementary

Data 2). A distinct, deeply rooted cluster of *S. pneumoniae* was formed that included 11 unencapsulated MLST types encompassing 89.3% of conjunctivitis isolates (Fig. 2). Only 1 sequence type that is encapsulated, ST199, caused more than 2 cases. This shows that conjunctivitis in the US is mainly caused by a closely related group of unencapsulated *S. pneumoniae* sequence types, although other strains can cause conjunctivitis, most likely as an extension of upper respiratory infection.

Traits of the unencapsulated conjunctivitis cluster

To determine whether strains from conjunctivitis that occur within the distinct branch of *S. pneumoniae* possess novel gene content, a total of 21 genomes of representatives of the major conjunctivitis-associated sequence types were sequenced (Supplementary Data 3). Diversity was maximized by selecting varying dates of isolation and sites of origin. Additionally, genomes of select encapsulated conjunctivitis strains were also sequenced, including ST199 (which caused 5 cases) and strains of sequence types ST632, ST667, ST180.

Genes encoding a total of 4,433 protein orthogroups were identified by OrthoMCL, 1,160 of which were present in single copy in all genomes. These core orthogroup genes were used to generate a single nucleotide polymorphism (SNP) based phylogenetic tree (Fig. 3). As for MLST, the SNP based core genome tree showed that strains isolated from epidemic conjunctivitis belong to a distinct, deeply resolved group that includes ST448, ST1186, ST344, ST1270 and ST2315. Lineages within this group were termed the Epidemic Conjunctivitis Cluster (ECC), since their genomes are highly related and these STs (ST448, ST344, ST1186) are associated with epidemic conjunctivitis outbreaks^{9,10,14,17,18}. Croucher and colleagues recently noted one group of unencapsulated strains (denoted Sequence Cluster 12 [SC12]), was the most divergent cluster from the main population in their study¹⁹. SC12 includes STs ST448 and ST344 associated with conjunctivitis. The phylogeny determined here was unchanged after filtering recombinogenic regions of DNA using BRAT NextGen²⁰, showing that recombination was not the main driver for this population structure. Encapsulated strains that are rarer causes of conjunctivitis (ST632, ST667, ST180 and ST199) are interspersed among strains that cause infection at other sites. The extent of divergence of shared genes within ECC genomes from those of other sites of infection was quantified²¹ (Supplementary Fig. 1). ECC genomes compared to each other exhibit an average nucleotide identity (ANI) value of 99.0% \pm 0.4, highlighting the very close relationship among ECC lineages. ECC strains are significantly more distantly related to those from other sites of infection (97.9% \pm 0.11 ANI, $p < 0.001$, Student's t-test).

ECC strains possess a distinct gene repertoire

Clustering of genomes based on similarities in gene content also places ECC strains into a well-resolved group, independently recapitulating phylogenetic structure (Supplementary Fig. 2) and supporting the hypothesis that the peculiar ocular tropism of ECC strains stems at least in part from novel gene content. As in the SNP-based phylogeny, strains that are rarer causes of conjunctivitis are interspersed among non-ocular *S. pneumoniae*. To identify genes that distinguish the ECC from other strains, because horizontal gene flow can complicate the analysis, we arbitrarily set gene presence in 80% or greater of ECC genomes, and $< 20\%$ of

the non-ECC comparator strains (or vice versa) as the cutoff. We found 230 genes that fulfill this enrichment criteria (Supplementary Data 4). Of these, 103 genes are in all ECC genomes and absent from all comparators. Conversely, 70 genes are missing from ECC that are present in 80–100% of non-ocular *S. pneumoniae* comparator genomes (Supplementary Data 5). Of those, 29 were found in all non-ocular genomes and no ECC strains. In patterns of gene presence and absence, encapsulated conjunctivitis strains were found to be most closely associated to those from other types of infection.

The comparatively large proportion of conjunctivitis caused by ST448 suggests that its genome may be especially refined to cause this disease (or alternatively, that among ECC lineages, ST448 is more widely distributed and abundant in nature). Seventeen orthogroups are unique to ST448 (Supplementary Data 6), including a hypothetical mobile element with closest relative in *S. mitis*. No genes are specifically missing from ST448 that in all other ECC genomes.

Evidence for large scale surface remodeling

In place of a capsule operon, all ECC strains we investigated possess the atypical locus that includes *aliC* (X231_0947) and *aliD* (X231_0948), but not the often associated *pspK* gene^{22,23}. However, in the absence of a capsule, a large number of novel surface features were found. Exclusive to ECC are two different Antigen I/II family adhesins (X231_1085 and X231_1187) (Supplementary Data 4), that appear to originate from *Streptococcus macedonicus* and *Streptococcus mitis* respectively (Fig. 4A). Owing to the presence of multiple SspB domains within these proteins, we termed them SspBC1 (X231_1085) and SspBC2 (X231_1187). SspB domain containing proteins have been shown to bind the human scavenger protein gp-340, which contributes to bacterial aggregation²⁴. To test for this functionality, a representative ECC strain (ST448), and a non-ECC encapsulated conjunctivitis strain that lacks SspBC1 and SspBC2 (ST199), were incubated with graded concentrations of gp-340. As shown in Figure 4B, the ST448 strain exhibited gp-340 concentration dependent aggregations. We also identified a unique gene inferred to encode a surface protein (X231_1186) termed here PspO. This surface protein gene is directly adjacent to that encoding SspBC2, suggesting a potential virulence island. PspO includes a C terminal glucan-binding domain and a surface exclusion domain.

Another gene predicted to affect the host/pathogen interface, that occurs exclusively in ECC strains, encodes a new divergent putative zinc metalloprotease (X231_0594), ZmpC2 (Supplementary Fig. 3A). The closest ortholog is in *S. pseudopneumoniae* IS7493, and it shares 31% amino acid sequence identity with the known ZmpC of *S. pneumoniae*, mainly in the Peptidase_M26_C domain (Supplementary Fig. 3A). Recently, a different, structurally related, atypical zinc metalloprotease C (*zmpC*, now termed ZmpC1) was identified in a *S. pneumoniae* conjunctivitis isolate, and was shown to cleave mucins from corneal epithelial cells^{25,26}. ZmpC1 (X231_0222) also occurs in 100% of ECC and 0% of comparators.

Additional surface related functions of potential relevance to conjunctivitis, include a putative sialidase (X231_0534), now termed NanO1. It shares 88% amino acid sequence identity with sialidase A (neuraminidase A) of *S. pseudopneumoniae*. The typical NanA of *S. pneumoniae*, which is carried by all non-ocular reference strains, has been displaced by

NanO1 in ECC (Supplementary Fig. 3B). Closer examination of the sequence surrounding *nanO1* identifies a second gene, also annotated as encoding a sialidase (referred to as NanO2, X231_0533), suggesting NanO1 and NanO2 from *S. pseudopneumoniae* recombinationally displaced wild type NanA (Supplementary Fig. 3C). Additionally, the neuraminidase allele NanC, found in approximately 51% of *S. pneumoniae* isolates from non-ocular sites²⁷, was not found within any ECC genome.

Choline binding proteins (Cbp) are important virulence factors that contribute to *S. pneumoniae* adhesion and transcytosis²⁸. All ECC genomes encode a novel, divergent Cbp (BM49_0273), CbpI1, that is most closely related to a variant in *S. pseudopneumoniae*. All ECC strains also encode a second Cbp variant (X231_0220, CbpI2) that is rare outside this cluster, occurring in 3 non-ocular comparator strains (AP200, G54, TIGR4)²⁸. CbpI1 and CbpI2 share a structurally related cysteine-rich secretory domain and a C-terminal choline-binding domain, and 48.3% overall amino acid sequence identity. Interestingly, CbpI2 and ZmpC1 are adjacent to one another within the ECC genomes.

S. pneumoniae genes with known roles in colonization and virulence include *cbpA*, *nanB*, *bgaA*, *strH*, *ply*, *hyl*, *plpA* (*aliA*), *psaABC*, *prtA*, *choP*, *pdgA*, *adr*, *spxB*, *amiA-amiF*, *msrA/B2*, and the two Pilus Islets^{29–31}. Choline binding protein A (CbpA), a main adhesin in respiratory infections and otherwise highly conserved in non-ocular strains^{31,32}, is substantially divergent in all ECC genomes. Two polymorphic forms of CbpA were found, CbpAC1 in ST448 and ST1186 genomes, and CbpAC2 in ST344, ST1270, and ST2315 (Fig. 5). Portions of CbpAC1 and CbpAC2 show little resemblance to CbpA, instead being closely related to the beta-antigen of *S. agalactiae*³³. The absence of CbpA from ECC strains was verified by Western blot using three different CbpA-specific monoclonal antibodies³⁴, indicating that the variant CbpA possesses a substantially different structure in the otherwise conserved key epitopes probed (Supplementary Fig. 4). The region of canonical CbpA that mediates binding to the eukaryotic polymeric Ig receptor (pIgR)³⁵, has been replaced by *S. agalactiae* domains that bind the Fc portion of IgA directly^{33,36}. The different variations in the divergence of CbpAC1 and CbpAC2 from CbpA suggest that variations of the hybrid CbpA locus evolved independently. Interestingly, in ECC the two-component system that regulates CbpA expression³⁷, also exhibits greater nucleotide sequence identity to its counterpart in *S. agalactiae* (Supplementary Fig. 4D). Differences in nucleotide sequence on either side of the two variant CbpAC loci support separate evolution of these determinants within ECC strains.

Two Pilus Islets have been described that contributing to *S. pneumoniae* epithelial cell adhesion^{29,30}. Neither pilus islet occurred in any ECC strain. Exoglycosidase BgaA is absent from all ECC isolates, as is a three gene PTS system (SP_0645 to SP_647) that occurs immediately adjacent *bgaA* in TIGR4, displaced by approximately 1 kb of sequence with high identity (>91%) to sequences in *S. mitis* and *S. pseudopneumoniae*. Otherwise, all other virulence-associated genes, including *nanB*, *strH*, *ply*, *hyl*, *plpA* (*aliA*), *psaABC*, *prtA*, *choP*, *pdgA*, *adr*, *spxB*, *amiA-amiF*, *msrA/B2* are present in all ECC strains, and are highly conserved (99.6% +/-0.3 inferred amino acid sequence identity to TIGR4).

Metabolic differences

All ECC strains encode a putative phosphoenolpyruvate-dihydroxyacetone phosphotransferase system (X231_1297 to X231_1300, Supplementary Data 4). Uniformly absent from ECC strains are operons for arginine metabolism (SP_2148 to SP_2151), and a fucose binding, uptake, and catabolic pathway (SP_2158 to SP_2170) (Supplementary Data 5). This block of metabolic functions has been displaced in ECC genomes with a 12.7 kb sequence that encodes, among other things, ZmpC2. Some ECC (ST448, ST344, ST1270) lack the *pia* operon mediating iron uptake, which in other strains has been linked to virulence in mouse models of pulmonary and systemic infection³⁸. Five other genes with putative annotations as amino acid transporters (SP_0111, SP_0112, and SP_0709 to SP_0711) are present in 100% of comparators, but uniformly absent in ECC, suggesting a substantially altered nutrient profile in the conjunctival mucosa (Supplementary Data 5).

Recombination and HGT

The occurrence of multigene blocks of difference suggests that movement of pathogenicity islands or other mobile elements were involved in the evolution of ECC. Of the 230 orthogroups enriched in ECC, 180 genes occur in 15 clusters (Table 1). The average G+C content (36.8% \pm 3.8) is lower than the rest of the genome (39.7%, $p < 0.01$, Student's *t*-test), which is common for mobile elements³⁹. Two clusters exclusive to ECC, an 18 kb predicted phage (cluster 9) and 13 kb encoding core genes (VirD/VirB/TrsE) of a Type IV secretion system (cluster 11), are adjacent. Interestingly, the cluster 9/cluster 11 element occurs at different locations within ECC STs, suggesting either independent acquisition, or internal movement. That it is mobile and presumably could be lost if not for selection, yet is retained, suggests that it may have a role in mediating the peculiar ocular tropism of ECC.

The majority (75%) of ECC carry resistance elements (Supplementary Fig. 5) consistent with antibiotic susceptibility⁴⁰. Macrolide resistance is the most common, and conferred by the Macrolide Efflux Genetic Assembly (MEGA) cassette in ST448 and ST1186, and by a Tn916-like integrative conjugative element (ICE) in ST344 and ST1270 (Supplementary Fig. 6). ST2315 was the only ECC isolate resistant to phenicols, which was conferred by an Spn11930-like ICE element.

Comparison to strains identified in asymptomatic carriage

Asymptomatic nasopharyngeal carriage generally precedes disease. To determine whether ECC strains were represented in large data sets from asymptomatic carriage, we looked for their occurrence in two recently reported studies^{19,41}. This expanded analysis substantiates the deeply rooted and well-clustered grouping of the ECC strains, but importantly, shows that ECC STs are distributed among additional closely related, unencapsulated strains isolated from the nasopharynxes that have not yet been associated with conjunctivitis (Fig. 6). It was thus of interest to compare the traits of ECC strains isolated from conjunctivitis to those isolated from the nasopharynx by investigating the presence or absence of a selection of newly identified ECC genes with a putative contribution to conjunctivitis pathogenesis. From the asymptomatic carriage data sets, we selected genome sequences of 96 strains that were of sequence types closely related to those that constituted the ECC group; and also diverse strains spread across the phylogenetic tree representing the most prevalent STs

associated with nasopharyngeal carriage regardless of their encapsulation status (Fig. 6, Supplemental Fig. 7 and Supplemental Data 7). All genes found to be enriched in ECC strains isolated from conjunctivitis were also found to be present within nasopharyngeal isolates of ST448, ST2315, ST344 genomes, indicating these strains are highly similar to those isolated from conjunctivitis, and supporting an infection model where asymptomatic carriage in the nasopharynx precedes ocular infection. Of the cumulative 3,701 nasopharyngeal isolates represented in the two nasopharyngeal surveys, no representatives of ST1186 or ST1270 were observed, in contrast to their occurrence at rates of 13/271 (4.8%) and 3/271 (1.1%) respectively in conjunctivitis cases, indicating their rarity among the circulating population despite their enrichment in cases of conjunctivitis.

Genes we identified as enriched in ECC strains isolated from conjunctivitis, *cbpAC1*, *cbpAC2*, and *nanO1/nanO2* were only found to occur among asymptomatic carriage strains of the same sequence types. Other genes we found enriched in ECC (*sspBC1*, *sspBC2*, *zmpC1*, *zmpC2*) occurred also in unencapsulated lineages that have not yet been observed in conjunctivitis, and the majority of these lineages are closely related phylogenetically to ECC strains (Fig. 6). Interestingly, some sequence types phylogenetically closely related to ECC strains (ST5126, ST4142, ST4139) were found to lack all ECC genes that were investigated. As these STs were not identified among conjunctivitis strains, their ability to cause this disease remains unknown.

Discussion

With a view toward understanding strain diversity and the molecular basis for virulence of *S. pneumoniae* in conjunctivitis, and to improving vaccine design to cover this disease, we characterized recent isolates from across the US. We found that nearly 90% of conjunctivitis cases were caused by five related STs (ST448, ST344, ST1186, ST1270, ST2315) that occur within a distinct cluster of the *S. pneumoniae* species (see Fig. 6 and Supplemental Fig. 7), a population structure supported by two recent reports^{19,41}. This divergence is characterized by novel gene content constituting approximately 10% of the genome. Although ECC strains possess a large amount of novel genes, shared genes exhibit an average nucleotide identity of 97.9% \pm 0.11 ANI with strains from other types of infection, and therefore ECC strains do not constitute a new species (ANI < 95%) by this definition^{21,42,19}.

We found genes *cbpAC1*, *cbpAC2*, *nanO1*, *nanO2* were only carried by STs that are associated with conjunctivitis (see Fig. 6 and Fig. 7). Other genes enriched in ECC, including the *sspBC* agglutinins, *zmpC1*, *zmpC2*, and the triose metabolic cassette, were found to be shared among a few closely related unencapsulated STs (ST6153, ST6691, ST6729, ST2996, ST1054, ST449) that have not been identified in cases of conjunctivitis, which may stem from the paucity of studies that have identified MLST types of *S. pneumoniae* causing conjunctivitis. These additional genes are largely absent in encapsulated and more distantly related unencapsulated genomes unrelated to conjunctivitis however (see Fig. 6 and Fig. 7). These findings suggest that some of the genes enriched in ECC are fundamental to the formation of the larger unencapsulated lineage to which ECC members belong (see Fig. 6 and Supplemental Fig. 7).

proteins mediate binding to human scavenger protein gp-340²⁴, which occurs in tears and on the ocular surface⁵².

All STs associated with conjunctivitis encoded a novel phage element (cluster 9/cluster 11). This element was also seen in closely related unencapsulated nasopharyngeal strains, whereas it was rarely found in more distantly related unencapsulated strains. Interestingly, this element is located at different sites in the genomes of the conjunctivitis associated sequence types, but is always consistent within an ST. This suggests that it was lacking from a common ancestor and has been acquired independently, or that it is internally mobile. There are no obvious adhesins or virulence traits encoded within this element, but it may contribute to biofilm formation as described for other phage elements in *S. pneumoniae*⁵³. Its presence within numerous nasopharyngeal STs suggests it may play a basic function in colonization for unencapsulated varieties of *S. pneumoniae*.

A unique metabolic feature profile was found among ECC and closely related strains, suggesting that their colonization ability is likely nutritionally distinct from that of strains associated with invasive infection. A phosphoenolpyruvate-dihydroxyacetone PTS gene cluster occurring in ECC and closely related nasopharyngeal strains and only 1 distantly related strain from otitis media (Hungary19A-6), (cluster 8), also found in *S. mitis* and *S. pseudopneumoniae*, suggests that the ability to metabolize Dha is important for mucosal surface colonization. DhaP was detected among the phosphorylated intermediate metabolites present on the ocular sclera and corneal tissues⁵⁴.

In addition to the gain of putative metabolic capabilities described above, all ST genomes associated with conjunctivitis lacked the ability to metabolize fucose, a sugar that decorates ocular glycans present in the glycocalyx of corneal epithelial cells⁴⁹. Fucosylated glycans coating mucins are known to promote bacterial colonization in the gut, serving as both adherence targets, as well as a carbon source^{55,56}. Specifically at the ocular surface, fucose residues have been implicated in the attachment of *P. aeruginosa* and *E. coli* to ocular epithelial cells⁴⁹. Moreover, application of exogenous fucose was shown to suppress inflammation in rabbit corneal and explanted human cornea models of wound healing⁵⁷. Nasopharyngeal STs closely related to ECC members (ST6691, ST6729, ST1054, ST449, ST2996, ST6153) were also found to lack the elements to metabolize fucose. These findings suggest the inability to metabolize fucose is irrelevant for colonizing the nasopharynx, but may confer an advantage at the ocular surface, potentially by promoting an anti-inflammatory environment and/or by preserving an important bacterial ligand.

While asymptomatic carriage in the nasopharyngeal cavity is likely to be a precursor to infection, ST448^{9,12,13,15,18} and related STs commonly isolated conjunctivitis were not highly prevalent in recent large scale surveys of asymptomatic *S. pneumoniae* carriage in the nasopharynx^{19,41}. Whereas ST448 was found to be by far the leading cause of conjunctivitis in this study as well as in others^{15,18}, it represented only 1.43% of 3,084 isolates found to be asymptotically carried by Chewapreecha *et al.*⁴¹, and 1.14% of nasopharyngeal isolates examined by Croucher *et al.*¹⁹. Indeed, there are four other unencapsulated STs found at similar or higher prevalence within the nasopharynxes (ST4133, ST4395, ST4965, ST4136 ranging from 1.43 to 2.92%), the most prevalent of which, ST4133, has not been reported as

a cause of conjunctivitis, is not closely related to the STs most commonly associated with conjunctivitis and does not encode the genes enriched in ECC that were searched, highlighting the point that it is not the simple lack of capsule that predisposes these strains to cause conjunctivitis. The four most common STs (ST4414, ST802, ST315, ST4209) in nasopharyngeal carriage are all encapsulated (a cumulative 19.98% of 3,084 isolates), and lack all ECC-associated genes (except for a phage (cluster 1) shared only in ST4414) and were not found among our collection of 271 conjunctivitis isolates. Similar findings were seen by Croucher *et al.*¹⁹, with 1.14% of nasopharyngeal isolates being ST448 (21st most common ST), in this case representing the most common unencapsulated ST recovered in their study. Taken together, these findings highlight that prevalence in the nasopharynx does not directly correlate with conjunctival infection, in further support of the hypothesis that genes unique to ECC genomes are critical for conjunctival infection.

It is unlikely that the unencapsulated cluster containing ECC members arose due to vaccine use, as has been speculated⁸, based upon the extent of divergence between ECC lineages investigated herein and non-ocular lineages (an average 27,754 \pm 1,831 SNPs). Based on a recent determination of *S. pneumoniae* mutation rate⁵⁸ (and assuming this measure is true for ECC members as well), the bifurcation between ECC and the main branch of the species took place approximately 8,400 years ago (8,385 \pm 553 years). That the rate of divergence measured for other *S. pneumoniae* also applies to ECC rates of change stems from a comparison of the distance between strains isolated from geographically and temporally related outbreaks in Maine and New Hampshire. With epidemiologic centers about 7 months apart, strains from the New Hampshire outbreak (ECC_1854, ECC_1910) differ from those from the Maine outbreak (ECC_0072, ECC_0083) 4.67 \pm 2.1 SNPs, a mutation rate of 1.43×10^{-6} substitutions per site per year, in agreement with previous calculations 1.57×10^{-6} substitutions per site per year⁵⁸. This dating is similar to estimates of clade divergence in *E. faecium*⁵⁹, and *S. aureus*⁶⁰, both of which were attributed to increasing urbanization. This suggests that in contrast to the ancestral line, there is an especially important role for person to person transmission in the propagation of either this lineage, or the branch associated with respiratory infection.

In summary, we found that 5 STs commonly associated with conjunctivitis (which accounted for 90% of *S. pneumoniae* conjunctivitis cases studied) belong to a distinct cluster of unencapsulated strains within the *S. pneumoniae* species. These strains are typified by substantially different features including elements exclusive to strains associated with conjunctivitis (CbpAC1, CbpAC2, NanO1, NanO2) that may contribute to their ocular tropism. Additional features were shared with only closely related unencapsulated varieties (e.g. ZmpC, SspBC2), or sporadically among distantly related unencapsulated strains (e.g. SspBC1). Currently 90% of the *S. pneumoniae* strains associated with conjunctivitis are not covered by existing vaccines. Furthermore, because of the extensive variation observed, vaccines under development that target conventional *S. pneumoniae* virulence traits (e.g. CbpA) may or may not provide coverage for preventing conjunctivitis. This knowledge of conserved and variant features occurring in the ECC members will be critical for future vaccine design strategies.

Methods

Bacterial strains

A large and comprehensive collection of 280 *S. pneumoniae* conjunctivitis strains were assembled from across the USA, including 271 isolates obtained from 72 different zip codes, as well as one isolate from New Delhi, India as part of a national, multicenter, passive surveillance study of bacterial conjunctivitis⁵⁻⁷. Also included were two conjunctivitis isolates (6 in total) from each large outbreak occurring at Dartmouth College^{10,12}, an elementary school in Maine^{13,17}, and a suburb of Minnesota⁹, as well as three other conjunctivitis isolates of unknown origin were obtained from the CDC Streptococcus Laboratory (Supplementary Data 1). Strains were cultured on 5% sheep blood agar plates (BD Biosciences, San Jose, CA) or in Todd Hewitt broth supplemented with 5% yeast extract, and incubated at 37 C in 5% CO₂. Bacterial isolates were confirmed as *S. pneumoniae* based on their hemolysis phenotype on blood agar plates, bile solubility, and susceptibility to optochin when grown in a 5% CO₂ atmosphere⁸.

Ocular isolate characterization by MLST and capsule typing

Multilocus sequence typing and capsule typing were performed on the 271 strains collected from the large US multicenter trial⁵⁻⁷ (Fig. 1B). Briefly, sequence types were determined based on sequences for *aroE*, *gdh*, *gki*, *recP*, *spi*, *xpt* and *ddl* genes⁶¹. The presence of capsule was determined with both OMNI serum, as well as the capsule type-specific Pneumotest-Latex serum, both obtained from the Statens Serum Institut (MiraVista Diagnostics, Indianapolis, IN). Initial capsule typing results for 50 selected isolates were confirmed by the Statens Serum Institut in Denmark. A preliminary report of the distribution of MLST types has been presented previously⁶².

Genome Sequencing

Strains isolated from three well-documented major US outbreaks in Maine, New Hampshire and Minnesota, as well as strains that were representative of the MLST sequence types most prevalent among the 271 strains collected from the multicenter US study, were selected for genome sequencing (Supplementary Data 1). Briefly, total DNA was purified from a 5 mL overnight culture using the DNeasy DNA extraction kit (Qiagen, Valencia, CA). Library preparation for Illumina sequencing by Illumina was carried out using the Nextera DNA Sample Preparation kit (Illumina, San Diego, CA), according to manufacturer's specifications. DNA quality was verified on a Bio-Tek Synergy 2 microplate reader (Winooski, VT) prior to quantification using a Qubit fluorometer and dsDNA High-Sensitivity assay kit (Invitrogen, Carlsbad, CA). A transposome was used to simultaneously fragment and append adapter sequences to 50 ng of DNA per sample, followed by addition of dual-index sequences in a limited-cycle PCR step. Quality and quantity of each sample library was measured on an Agilent Technologies 2100 Bioanalyzer (Santa Clara, CA), with a target fragment size μ 300bp. The genomes of strains ECC_0072, ECC_0083, ECC_1854, ECC_1910, SC_0381, and SC_0391 were sequenced at the St. Jude Children's Hospital Hartwell Center for Bioinformatics and Biotechnology, Memphis, TN on an Illumina GAXII sequencer, according to manufacture's specifications. For all other genomes, libraries were normalized to 2 nM, multiplexed and subjected to either 150, 200 or 250 bp paired end

sequencing on an Illumina MiSeq Personal Sequencer at the Mass. Eye and Ear Infirmiry Ocular Genomics Institute (Boston, MA), according to manufacturer's specifications.

Genome assemblies and annotation

Sequence reads were assembled *de novo* utilizing CLC Genomics Workbench v4.9 (CLC Bio, Cambridge, MA) (Supplementary Data 3). On average, 3.7 million high-quality paired-end reads were collected for each strain, representing > 240-fold coverage of the μ 2.1 Mb genomes. Sequence reads below a quality score of 25 at any position were excluded from further analyses. All genomes compared in this study (Supplementary Data 2) were annotated using the Rapid Annotation using Subsystem Technology (RAST) server⁶³, and Glimmer v.3⁶⁴, with comparison to family profiles in the FIGfam (protein families generated by the Fellowship for Interpretation of Genomes (FIG)) release 63 database. Wherever possible, manual search of the PFAM⁶⁵ database was used to assign functions to genes annotated as hypothetical.

Orthogroups and gene families

Orthogroups were calculated across all of the genomes in our dataset using OrthoMC⁶⁶, with a BLAST e-value of 10^{-5} and an inflation index of 2.5. Orthogroups contain orthologs, which are vertically inherited genes that likely have the same function, and also possibly paralogs, which are duplicated genes that may have different function.

Phylogenic and ANI analyses

SNP-based phylogeny based upon MLST allele sequence and single copy core alignment was generated using PhyML and statistics were calculated for 1000 bootstrap replicates⁶⁷. To generate a MLST-based tree, DNA sequences for the seven MLST loci were concatenated and aligned for each of the 31 sequence types represented in the conjunctivitis isolates (Fig. 2) and the 26 non-ocular reference genomes (Supplementary Data 2).

A phylogenetic tree of all genomes in our dataset, including the 21 genomes newly sequenced as well as 26 reference genomes (Supplementary Data 2), was generated using all 1160 single-copy core orthogroups, including *Streptococcus mitis* strain B6 as an outgroup. BRAT NextGen analysis was conducted on the 1160 single-copy core orthogroup alignment of the 47 *S. pneumoniae* genomes to identify filter out recombinogenic regions^{19,68}. Percent average nucleotide identity (ANI) was calculated by dividing the number of identical nucleotide residues in shared genes by the total number of nucleotides in shared genes²¹. Shared gene content between strains in pairwise genome comparisons was generated by searching the CDS predictions from one genome annotation against the annotations of the second genome and conserved genes were identified by BLAST matching > 60% overall sequence identity²¹.

Identification of antibiotic resistance genes

The Resfinder database was used to identify candidate antibiotic resistance genes as described previously⁶⁹. For a subset of the isolates, susceptibility was tested in microtiter plates and minimum inhibitory concentrations (MICs) were determined by broth

microdilution according to the procedure recommended by the Clinical and Laboratory Standards Institute (CLSI).

Western Blot

Logarithmically growing cells ($OD_{600}=0.5$) were pelleted by centrifugation and subjected to lysis in 0.1% Triton X-100. To ensure equal loading, protein concentration was determined for each lysate via absorbance at 280 nm and loaded accordingly. Duplicate gels stained with Coomassie were used to confirm equivalent loading. Lysates were run on 10% NuPAGE Bis-Tris gels (Invitrogen). Proteins were subsequently transferred to PVDF membranes by Western Blot. CbpA was detected using 3 monoclonal antibodies (1:5000) in PBS-T/5% non-fat dry milk (NFDm). The three monoclonal antibodies (14A3, 3G12, and 3H11) recognize the highly conserved loop regions in the R2 domain of CbpA and were generated as previously described³⁴. Pneumolysin was detected using rabbit polyclonal serum generated against recombinant pneumolysin. Secondary HRP-conjugated antibodies (Biorad, Hercules, CA) were used at 1:5000 in PBS-T/5% NFDm. Images of the complete Western blots are provided in Supplementary Figure 8.

Aggregation assays with gp-340

Bacterial isolates (ST448, ECC_3540; and ST199, SC_3526) were cultured over night in Todd Hewitt broth, pelleted after centrifugation ($5000 \times g$ for 10 minutes), washed twice in PBS and resuspended to an optical density at $OD_{600} = 0.6$ in PBS. Bacterial suspensions (300 μ l) were incubated in 5 ml culture tubes in an orbital shaker at 300 RPM for 1 h at 37°C with 0, 0.5 and 1.0 μ g/ml of purified gp-340 (DMBT-1 recombinant human protein, Life Technologies). Tubes were then rested for 1 h at 37°C to allow bacterial aggregates to settle. Gram staining was performed for each reaction to demonstrate bacterial aggregation and representative images were acquired using an Olympus BX60 microscope.

Characterization of ECC genes in nasopharyngeal genomes

Additional genomes of nasopharyngeal isolates were analyzed for genes found in our original dataset to be specific to ECC genomes including: (a) 29 additional representatives of strains known to be associated with ECC (23 ST448, 4 SLV448, 1 ST344, 1 ST2315), (b) 19 representatives of STs closely related to those associated with ECC, (c) 44 unencapsulated STs not closely related to ECC members were analyzed (Supplementary Data 7), (d) 4 encapsulated STs that were most prevalent in Chewapreecha *et al.*⁴¹. This included all unencapsulated nasopharyngeal genomes in Croucher *et al.*¹⁹ (16 genomes) and 8 draft genomes of nasopharyngeal isolates currently available from either the NCBI GenBank or European Nucleotide Archive (ENA), including 5 genomes newly deposited to NCBI GenBank⁷⁰. When available, we maximized the diversity of this set by downloading several representatives, spanning various dates of isolation, or when additional information on strain diversity was available (e.g. Bayesian Analysis of Population Structure⁴¹). Genomes were downloaded from the ENA read archive and assembled using CLC Genomics Workbench as described above. All together an additional 96 genomes of nasopharyngeal origin were selected to serve as a local BLAST database, which was used to

search (>80% query coverage, >80% nucleotide identity) for the presence of genes identified as specific to the ECC genes in our original dataset (Supplemental Data 7).

Supplementary Material

Refer to Web version on PubMed Central for supplementary material.

Acknowledgements

Portions of this project were supported by NIH grants EY024285, Molecular Basis for Ocular Surface Tropism in Conjunctivitis, and by the Harvard-wide Program on Antibiotic Resistance, AI083214. HHSN272200900018C supported the involvement of AM-M, AMM. Additional support for this project was obtained from the ALSAC organization of St. Jude Children's Research Hospital (JWR, CB, RAC, EIT). Additionally, portions of this project were supported by Bausch and Lomb, Inc. (CMS, WH, TWM, MSG). MDV was supported in part by NIH fellowship through EY007145. We gratefully thank Drs. F. Lebreton, D. Van Tyne and M. Martin for helpful comments throughout the course of this work and during manuscript preparation. Funding agencies had no role in study design, data analysis, decision to publish or preparation of the manuscript. PJMB was supported by a grant from the Coordenação de Aperfeiçoamento de Pessoal de Nível Superior, Brazil (CAPES #9775-13-7).

References

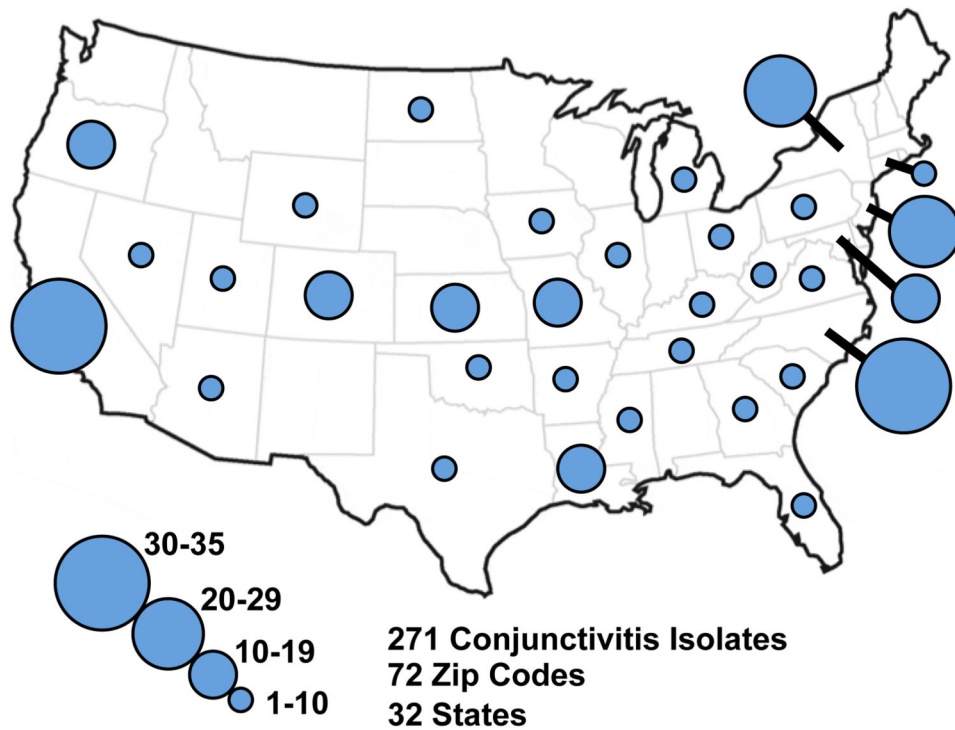
1. Tuomanen EI, Austrian R, Masure HR. Pathogenesis of pneumococcal infection. *N Engl J Med.* 1995; 332:1280–1284. [PubMed: 7708073]
2. Vernatter J, Pirofski LA. Current concepts in host-microbe interaction leading to pneumococcal pneumonia. *Curr Opin Infect Dis.* 2013; 26:277–283. [PubMed: 23571695]
3. Farrell DJ, Klugman KP, Pichichero M. Increased antimicrobial resistance among nonvaccine serotypes of *Streptococcus pneumoniae* in the pediatric population after the introduction of 7-valent pneumococcal vaccine in the United States. *Pediatr Infect Dis J.* 2007; 26:123–128. [PubMed: 17259873]
4. Buznach N, Dagan R, Greenberg D. Clinical and bacterial characteristics of acute bacterial conjunctivitis in children in the antibiotic resistance era. *Pediatr Infect Dis J.* 2005; 24:823–828. [PubMed: 16148850]
5. Karpecki P, et al. Besifloxacin ophthalmic suspension 0.6% in patients with bacterial conjunctivitis: A multicenter, prospective, randomized, double-masked, vehicle-controlled, 5-day efficacy and safety study. *Clin Ther.* 2009; 31:514–526. [PubMed: 19393842]
6. McDonald MB, et al. Efficacy and safety of besifloxacin ophthalmic suspension 0.6% compared with moxifloxacin ophthalmic solution 0.5% for treating bacterial conjunctivitis. *Ophthalmology.* 2009; 116:1615–1623. e1611. [PubMed: 19643483]
7. Tepedino ME, et al. Phase III efficacy and safety study of besifloxacin ophthalmic suspension 0.6% in the treatment of bacterial conjunctivitis. *Curr Med Res Opin.* 2009; 25:1159–1169. [PubMed: 19323612]
8. Haas W, Hesje CK, Sanfilippo CM, Morris TW. High proportion of nontypeable *Streptococcus pneumoniae* isolates among sporadic, nonoutbreak cases of bacterial conjunctivitis. *Curr Eye Res.* 2011; 36:1078–1085. [PubMed: 21988450]
9. Buck JM, et al. A community outbreak of conjunctivitis caused by nontypeable *Streptococcus pneumoniae* in Minnesota. *Pediatr Infect Dis J.* 2006; 25:906–911. [PubMed: 17006286]
10. Martin M, et al. An outbreak of conjunctivitis due to atypical *Streptococcus pneumoniae*. *N Engl J Med.* 2003; 348:1112–1121. [PubMed: 12646668]
11. Shayegani M, Parsons LM, Gibbons WE Jr, Campbell D. Characterization of nontypable *Streptococcus pneumoniae*-like organisms isolated from outbreaks of conjunctivitis. *J Clin Microbiol.* 1982; 16:8–14. [PubMed: 6809792]
12. (CDC), C. f. D. C. a. P. Outbreak of bacterial conjunctivitis at a college--New Hampshire, January-March, 2002. *MMWR Morb Mortal Wkly Rep.* 2002; 51:205–207. [PubMed: 11922188]
13. (CDC), C. f. D. C. a. P. Pneumococcal conjunctivitis at an elementary school--Maine, September 20-December 6, 2002. *MMWR Morb Mortal Wkly Rep.* 2003; 52:64–66. [PubMed: 12578323]

14. Crum NF, Barrozo CP, Chapman FA, Ryan MA, Russell KL. An outbreak of conjunctivitis due to a novel unencapsulated *Streptococcus pneumoniae* among military trainees. *Clin Infect Dis*. 2004; 39:1148–1154. [PubMed: 15486838]
15. Hanage WP, Kaijalainen T, Saukkoriipi A, Rickcord JL, Spratt BG. A successful, diverse disease-associated lineage of nontypeable pneumococci that has lost the capsular biosynthesis locus. *J Clin Microbiol*. 2006; 44:743–749. [PubMed: 16517849]
16. Enright MC, Spratt BG. A multilocus sequence typing scheme for *Streptococcus pneumoniae*: identification of clones associated with serious invasive disease. *Microbiology*. 1998; 144(Pt 11): 3049–3060. [PubMed: 9846740]
17. Zegans ME, et al. Clinical features, outcomes, and costs of a conjunctivitis outbreak caused by the ST448 strain of *Streptococcus pneumoniae*. *Cornea*. 2009; 28:503–509. [PubMed: 19421049]
18. Marimon JM, Ercibengoa M, Garcia-Arenzana JM, Alonso M, Perez-Trallero E. *Streptococcus pneumoniae* ocular infections, prominent role of unencapsulated isolates in conjunctivitis. *Clin Microbiol Infect*. 2013; 19:E298–E305. [PubMed: 23517475]
19. Croucher NJ, et al. Population genomics of post-vaccine changes in pneumococcal epidemiology. *Nat Genet*. 2013; 45:656–663. [PubMed: 23644493]
20. Martinen P, et al. Detection of recombination events in bacterial genomes from large population samples. *Nucleic Acids Res*. 2012; 40:e6. [PubMed: 22064866]
21. Konstantinidis KT, Tiedje JM. Genomic insights that advance the species definition for prokaryotes. *Proc Natl Acad Sci U S A*. 2005; 102:2567–2572. [PubMed: 15701695]
22. Keller LE, et al. PspK of *Streptococcus pneumoniae* increases adherence to epithelial cells and enhances nasopharyngeal colonization. *Infect Immun*. 2013; 81:173–181. [PubMed: 23115034]
23. Park IH, et al. Nontypeable pneumococci can be divided into multiple cps types, including one type expressing the novel gene pspK. *MBio*. 2012; 3
24. Jakubovics NS, Stromberg N, van Dolleweerd CJ, Kelly CG, Jenkinson HF. Differential binding specificities of oral streptococcal antigen I/II family adhesins for human or bacterial ligands. *Mol Microbiol*. 2005; 55:1591–1605. [PubMed: 15720563]
25. Govindarajan B, et al. A metalloproteinase secreted by *Streptococcus pneumoniae* removes membrane mucin MUC16 from the epithelial glycocalyx barrier. *PLoS One*. 2012; 7:e32418. [PubMed: 22412870]
26. Menon BB, Govindarajan B. Identification of an atypical zinc metalloproteinase, ZmpC, from an epidemic conjunctivitis-causing strain of *Streptococcus pneumoniae*. *Microb Pathog*. 2013; 56:40–46. [PubMed: 23168398]
27. Pettigrew MM, Fennie KP, York MP, Daniels J, Ghaffar F. Variation in the presence of neuraminidase genes among *Streptococcus pneumoniae* isolates with identical sequence types. *Infect Immun*. 2006; 74:3360–3365. [PubMed: 16714565]
28. Gosink KK, Mann ER, Guglielmo C, Tuomanen EI, Masure HR. Role of novel choline binding proteins in virulence of *Streptococcus pneumoniae*. *Infect Immun*. 2000; 68:5690–5695. [PubMed: 10992472]
29. Bagnoli F, et al. A second pilus type in *Streptococcus pneumoniae* is prevalent in emerging serotypes and mediates adhesion to host cells. *J Bacteriol*. 2008; 190:5480–5492. [PubMed: 18515415]
30. Hilleringmann M, et al. Molecular architecture of *Streptococcus pneumoniae* TIGR4 pili. *Embo J*. 2009; 28:3921–3930. [PubMed: 19942854]
31. Mook-Kanamori BB, Geldhoff M, van der Poll T, van de Beek D. Pathogenesis and pathophysiology of pneumococcal meningitis. *Clin Microbiol Rev*. 2011; 24:557–591. [PubMed: 21734248]
32. Luo R, et al. Solution structure of choline binding protein A, the major adhesin of *Streptococcus pneumoniae*. *Embo J*. 2005; 24:34–43. [PubMed: 15616594]
33. Jerlstrom PG, Chhatwal GS, Timmis KN. The IgA-binding beta antigen of the c protein complex of Group B streptococci: sequence determination of its gene and detection of two binding regions. *Mol Microbiol*. 1991; 5:843–849. [PubMed: 1857207]
34. Mann B, et al. Broadly Protective Protein-Based Pneumococcal Vaccine Composed of Pneumolysin Toxoid-CbpA Peptide Recombinant Fusion Protein. *J Infect Dis*. 2013

35. Zhang JR, et al. The polymeric immunoglobulin receptor translocates pneumococci across human nasopharyngeal epithelial cells. *Cell*. 2000; 102:827–837. [PubMed: 11030626]
36. Jerlstrom PG, Talay SR, Valentin-Weigand P, Timmis KN, Chhatwal GS. Identification of an immunoglobulin A binding motif located in the beta-antigen of the c protein complex of group B streptococci. *Infect Immun*. 1996; 64:2787–2793. [PubMed: 8698509]
37. Rosch JW, Mann B, Thornton J, Sublett J, Tuomanen E. Convergence of regulatory networks on the pilus locus of *Streptococcus pneumoniae*. *Infect Immun*. 2008; 76:3187–3196. [PubMed: 18443093]
38. Brown JS, Gilliland SM, Spratt BG, Holden DW. A locus contained within a variable region of pneumococcal pathogenicity island I contributes to virulence in mice. *Infect Immun*. 2004; 72:1587–1593. [PubMed: 14977965]
39. Frost LS, Leplae R, Summers AO, Toussaint A. Mobile genetic elements: the agents of open source evolution. *Nat Rev Microbiol*. 2005; 3:722–732. [PubMed: 16138100]
40. Haas W, Gearing LS, Hesje CK, Sanfilippo CM, Morris TW. Microbiological etiology and susceptibility of bacterial conjunctivitis isolates from clinical trials with ophthalmic, twice-daily besifloxacin. *Adv Ther*. 2012; 29:442–455. [PubMed: 22644963]
41. Chewapreecha C, et al. Dense genomic sampling identifies highways of pneumococcal recombination. *Nat Genet*. 2014
42. Konstantinidis KT, Ramette A, Tiedje JM. The bacterial species definition in the genomic era. *Philos Trans R Soc Lond B Biol Sci*. 2006; 361:1929–1940. [PubMed: 17062412]
43. Michel JL, Madoff LC, Kling DE, Kasper DL, Ausubel FM. Cloned alpha and beta C-protein antigens of group B streptococci elicit protective immunity. *Infect Immun*. 1991; 59:2023–2028. [PubMed: 1674738]
44. Kim HK, Thammavongsa V, Schneewind O, Missiakas D. Recurrent infections and immune evasion strategies of *Staphylococcus aureus*. *Curr Opin Microbiol*. 2012; 15:92–99. [PubMed: 22088393]
45. Fagan PK, Reinscheid D, Gottschalk B, Chhatwal GS. Identification and characterization of a novel secreted immunoglobulin binding protein from group A streptococcus. *Infect Immun*. 2001; 69:4851–4857. [PubMed: 11447160]
46. Lofling J, Vimberg V, Battig P, Henriques-Normark B. Cellular interactions by LPxTG-anchored pneumococcal adhesins and their streptococcal homologues. *Cell Microbiol*. 2011; 13:186–197. [PubMed: 21199258]
47. Wells PA, Hazlett LD. Complex carbohydrates at the ocular surface of the mouse: an ultrastructural and cytochemical analysis. *Exp Eye Res*. 1984; 39:19–35. [PubMed: 6207040]
48. Hazlett LD, Moon M, Berk RS. In vivo identification of sialic acid as the ocular receptor for *Pseudomonas aeruginosa*. *Infect Immun*. 1986; 51:687–689. [PubMed: 3080374]
49. Royle L, et al. Glycan structures of ocular surface mucins in man, rabbit and dog display species differences. *Glycoconj J*. 2008; 25:763–773. [PubMed: 18465222]
50. Donati C, et al. Structure and dynamics of the pan-genome of *Streptococcus pneumoniae* and closely related species. *Genome Biol*. 2010; 11(R107)
51. Brady LJ, et al. The changing faces of Streptococcus antigen I/II polypeptide family adhesins. *Mol Microbiol*. 2010; 77:276–286. [PubMed: 20497507]
52. Jumblatt MM, et al. Glycoprotein 340 in normal human ocular surface tissues and tear film. *Infect Immun*. 2006; 74:4058–4063. [PubMed: 16790779]
53. Carolo M, Frias MJ, Pinto FR, Melo-Cristino J, Ramirez M. Prophage spontaneous activation promotes DNA release enhancing biofilm formation in *Streptococcus pneumoniae*. *PLoS One*. 2010; 5:e15678. [PubMed: 21187931]
54. Sachedina S, Greiner JV, Glonek T. Phosphatic intermediate metabolites of the porcine ocular tunica fibrosa. *Exp Eye Res*. 1991; 52:253–260. [PubMed: 2015855]
55. Pacheco AR, et al. Fucose sensing regulates bacterial intestinal colonization. *Nature*. 2012; 492:113–117. [PubMed: 23160491]
56. Stahl M, et al. L-fucose utilization provides *Campylobacter jejuni* with a competitive advantage. *Proc Natl Acad Sci U S A*. 2011; 108:7194–7199. [PubMed: 21482772]

57. Isnard N, Bourles-Dagonet F, Robert L, Renard G. Studies on corneal wound healing Effect of fucose on iodine vapor-burnt rabbit corneas. *Ophthalmologica*. 2005; 219:324–333. [PubMed: 16286790]
58. Croucher NJ, et al. Rapid pneumococcal evolution in response to clinical interventions. *Science*. 2011; 331:430–434. [PubMed: 21273480]
59. Lebreton F, et al. Emergence of epidemic multidrug-resistant *Enterococcus faecium* from animal and commensal strains. *MBio*. 2013; 4
60. Weinert LA, et al. Molecular dating of human-to-bovid host jumps by *Staphylococcus aureus* reveals an association with the spread of domestication. *Biol Lett*. 2012; 8:829–832. [PubMed: 22628096]
61. Maiden MC, et al. Multilocus sequence typing: a portable approach to the identification of clones within populations of pathogenic microorganisms. *Proc Natl Acad Sci U S A*. 1998; 95:3140–3145. [PubMed: 9501229]
62. Sanfilippo, CM.; Haas, W.; Hesje, CK.; Morris, TW. Association for Research in Vision and Ophthalmology (ARVO). Florida: Fort Lauderdale; 2012.
63. Aziz RK, et al. The RAST Server: rapid annotations using subsystems technology. *BMC Genomics*. 2008; 9:75. [PubMed: 18261238]
64. Delcher AL, Harmon D, Kasif S, White O, Salzberg SL. Improved microbial gene identification with GLIMMER. *Nucleic Acids Res*. 1999; 27:4636–4641. [PubMed: 10556321]
65. Finn RD, et al. The Pfam protein families database. *Nucleic Acids Res*. 2008; 36:D281–D288. [PubMed: 18039703]
66. Li L, Stoeckert CJ Jr, Roos DS. OrthoMCL: identification of ortholog groups for eukaryotic genomes. *Genome Res*. 2003; 13:2178–2189. [PubMed: 12952885]
67. Guindon S, et al. New algorithms and methods to estimate maximum-likelihood phylogenies: assessing the performance of PhyML 3.0. *Syst Biol*. 2010; 59:307–321. [PubMed: 20525638]
68. Corander J, Waldmann P, Martinen P, Sillanpaa MJ. BAPS 2: enhanced possibilities for the analysis of genetic population structure. *Bioinformatics*. 2004; 20:2363–2369. [PubMed: 15073024]
69. Zankari E, et al. Identification of acquired antimicrobial resistance genes. *J Antimicrob Chemother*. 2012; 67:2640–2644. [PubMed: 22782487]
70. Keller LE, et al. Draft Genome Sequences of Five Multilocus Sequence Types of Nonencapsulated *Streptococcus pneumoniae* . *Genome Announc*. 2013; 1

a



b

Sequence type (Number of cases) % Total								
ST448	(182)	67.16	ST42	(1)	0.37	ST508	(1)	0.37
ST344	(24)	8.86	ST62	(1)	0.37	ST568	(1)	0.37
ST1186	(13)	4.80	ST63	(1)	0.37	ST995	(1)	0.37
ST2315	(12)	4.43	ST190	(1)	0.37	ST1176	(1)	0.37
ST199	(5)	1.85	ST320	(1)	0.37	ST1540	(1)	0.37
ST2011	(4)	1.48	ST338	(1)	0.37	ST3137	(1)	0.37
ST1270	(3)	1.11	ST392	(1)	0.37	ST4149	(1)	0.37
ST1768	(2)	0.74	ST395	(1)	0.37	ST6132	(1)	0.37
ST3064	(2)	0.74	ST452	(1)	0.37	ST6961	(1)	0.37
ST558	(2)	0.74	ST458	(1)	0.37			
ST816	(2)	0.74	ST460	(1)	0.37			

Figure 1. Location and MLST profile of conjunctivitis isolates

271 isolates of *S. pneumoniae* from diagnosed cases of conjunctivitis. (a) Number and geographic location of isolates. (b) Frequency of MLST types among conjunctivitis isolates.

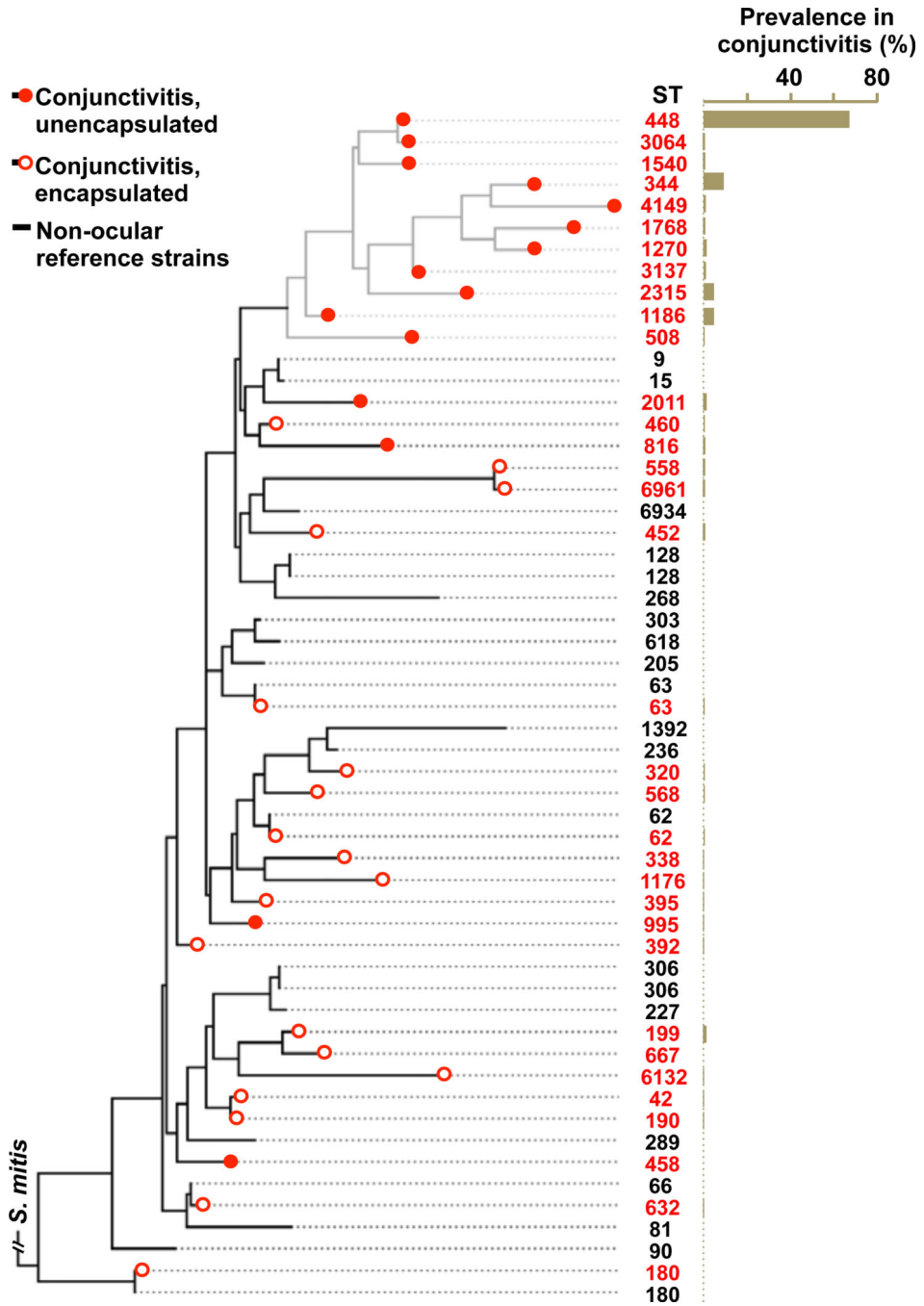


Figure 2. MLST-based phylogenetic relationships among conjunctivitis strains
 SNP-based tree based on a concatenation of MLST loci, with prevalence in conjunctivitis for each ST.

Author Manuscript

Author Manuscript

Author Manuscript

Author Manuscript

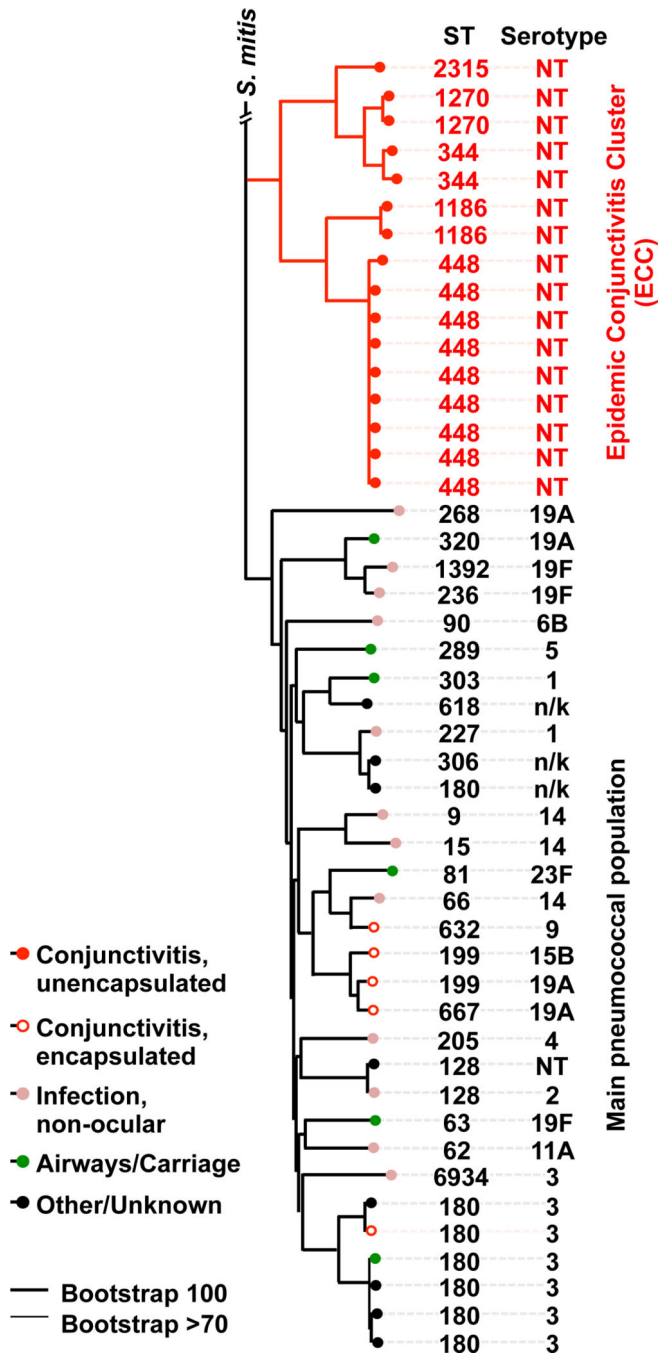


Figure 3. ECC strains belong to a well resolved group of the species *S. pneumoniae*
 A PhyML SNP-based tree based on the concatenated alignments of 1160 single copy core genes (for strain identities, see Supplementary Data 2). Bootstrapping was performed with 1000 iterations.

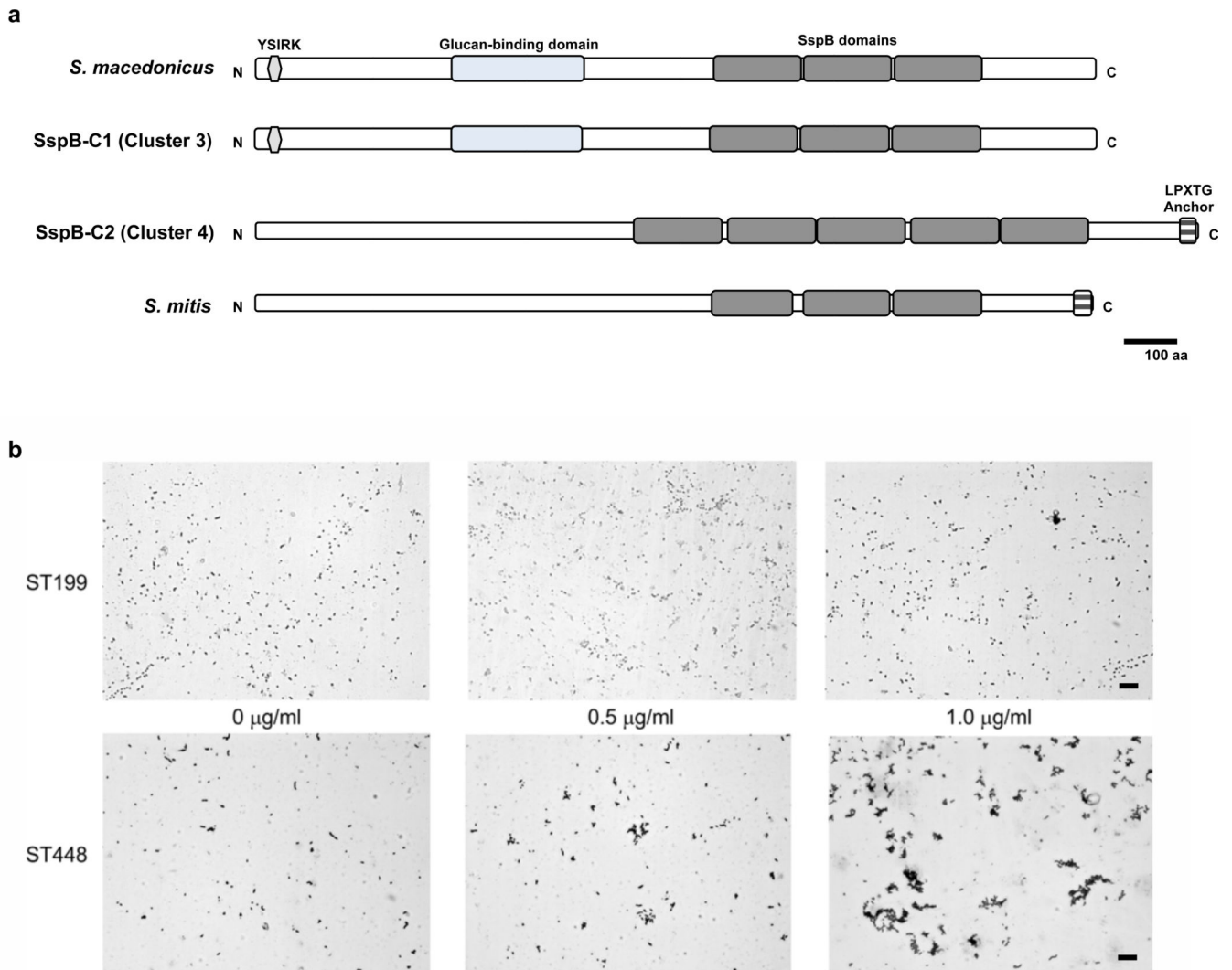


Figure 4. Homologs of agglutinin receptors in ECC

(a) SspB-C1 and SspB-C2 agglutinins exhibit identity to glucan binding and SspB domains in orthologs from *S. macedonicus* or *S. mitis* (b) Aggregation of ST448 (ECC_3540) and ST199 (SC_3526) isolates after addition of 0.5 µg/ml and 1.0 µg/ml of gp340 visualized by Gram staining. Scale bar represents 20µm.

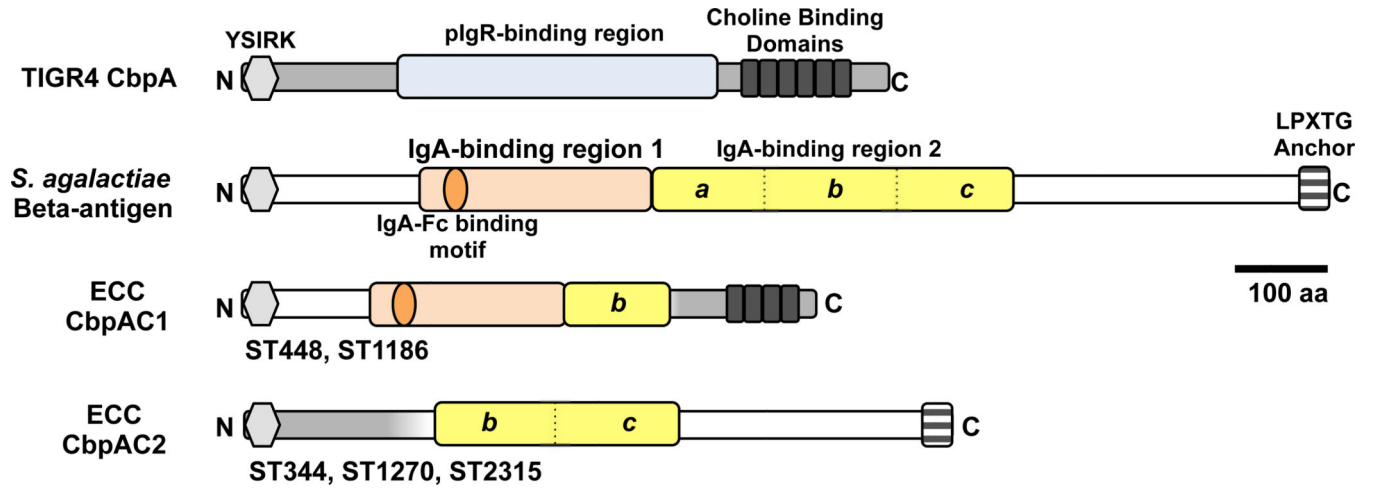


Figure 5. ECC genomes encode an atypical CbpA

Canonical CbpA of TIGR4 compared to those in ECC genomes, and the inferred donor, *S. agalactiae* C beta-antigen. Sequence most likely deriving from *S. pneumoniae* (grey) and *S. agalactiae* (white). Domains relevant to pIgR or IgA-binding are highlighted. The IgA-binding domain of *S. agalactiae* beta-antigen is duplicated, and domain 2 has been divided into portions (a, b, c) for purposes of illustrating the likely origins of fragments that share amino acid sequence identity in ECC variants.

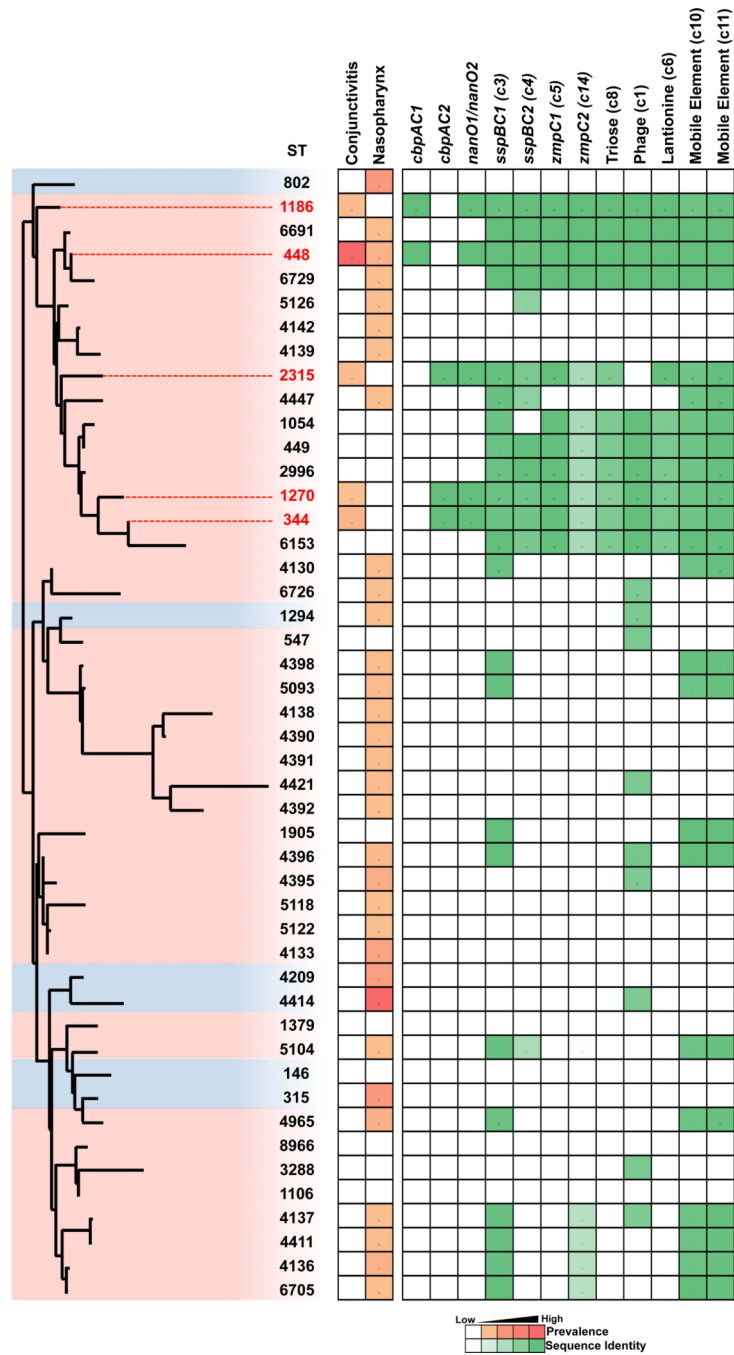


Figure 6. Presence of ECC genes in genomes of nasopharyngeal isolates

All STs representative of unencapsulated strains (pink highlight), and the most prevalent encapsulated strains (blue highlight), from two recent large scale surveys of asymptomatic nasopharyngeal carriage^{19,41}, compared to ECC members associated with conjunctivitis (red text and line extension), shown in a PhyML SNP-based tree based on the concatenated alignments of MLST alleles. Bootstrapping was performed with 1000 iterations. Prevalence in conjunctivitis (this study) and nasopharyngeal carriage⁴¹ is shown. Percent presence and

sequence identity of gene (*gene*, cluster number) or cluster (predicted function, cluster number) is denoted with green boxes.

Author Manuscript

Author Manuscript

Author Manuscript

Author Manuscript

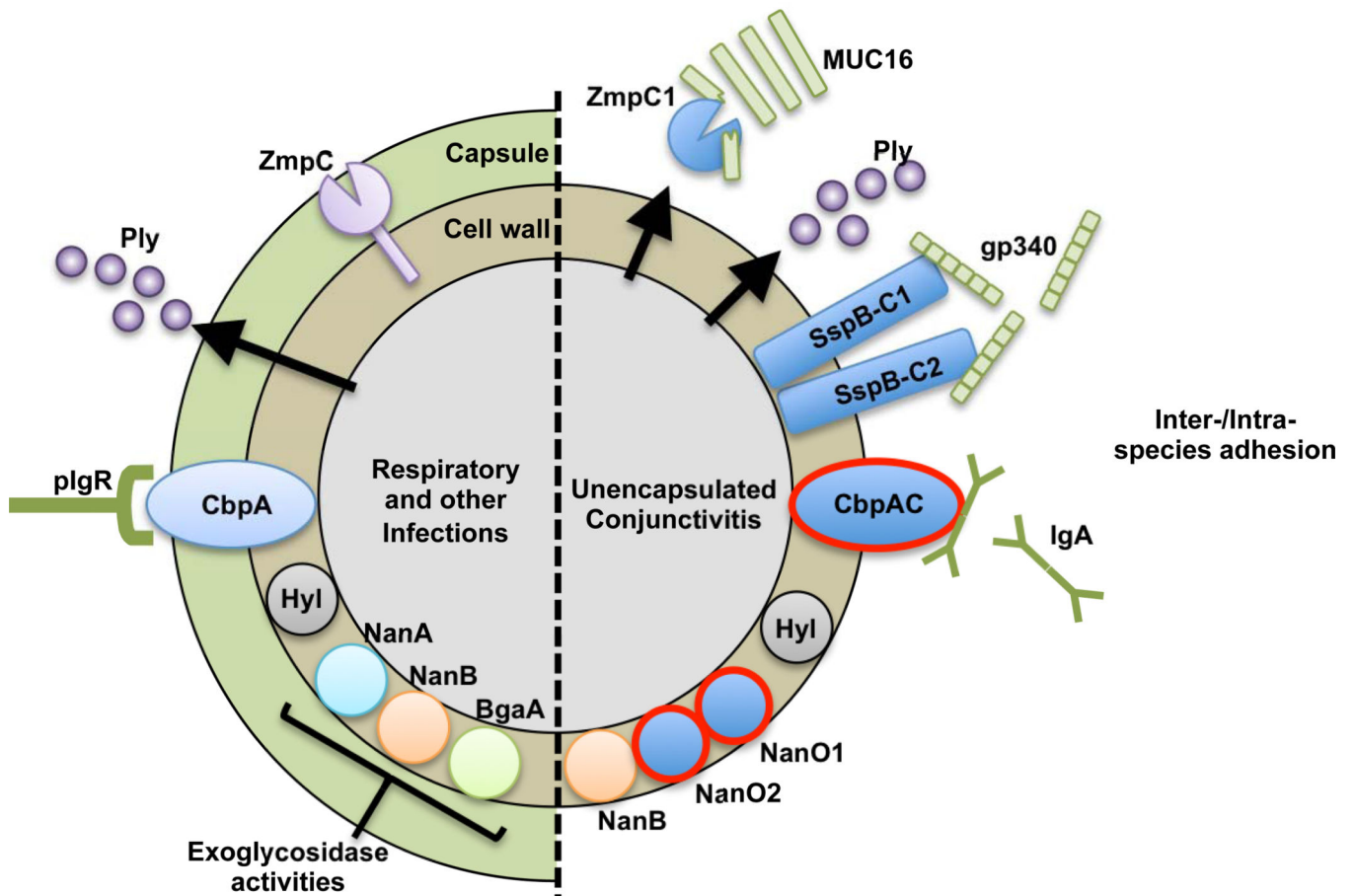


Figure 7. Virulence factor differences between invasive and ECC strains

New traits found within ECC and closely related genomes are shown in solid blue, with those unique to STs associated with conjunctivitis highlighted with red outline. CbpAC1 and CbpAC2 are shown as CbpAC since ECC strains express one or the other, but not both. Predicted ligands for SspBC1, SspBC2, and CbpAC are shown. Host-derived molecules are illustrated in green. Arrows indicate secreted products.

Table 1

Gene clusters enriched in ECC genomes.

Cluster ¹	Putative Function ²	Putative Origin ³	Size (kb)	%GC
2	Atypical capsule locus of NT pneumococci	<i>S. pneumoniae</i>	6.1	37.9
5	ZmpC1 specific to conjunctivitis genomes, CbpI2	<i>S. pneumoniae</i>	11.4	38.3
14	ZmpC2	<i>S. pseudopneumoniae</i>	10.2	40.1
3	SspBC1 Agglutinin receptor	<i>S. macedonicus</i>	15.4	40.8
4	SspBC2 Agglutinin receptor from <i>S. mitis</i> , Unknowns from <i>S. oligofermentans</i> ^a	<i>S. mitis</i> , <i>S. oligofermentans</i>	17.7	36.4
10	Mobile Genetic Element ^a	<i>S. oligofermentans</i>	16.8	35.9
9	Phage ^b	non- <i>S. pneumoniae</i> , <i>Streptococcus</i> sp.	18.7	37.0
11	Mobile Genetic Element containing putative Type IV secretory system genes ^b	<i>S. macedonicus</i>	13.2	42.6
8	Metabolic cassette, triose metabolism	<i>S. pneumoniae</i>	4.4	38.3
1	Phage element, intact, containing toxin/antitoxin in ST448/ST1186	<i>S. pneumoniae</i>	33.4	39.4
6	Lanthionine biosynthesis genes and unknowns from <i>S. oralis</i>	<i>S. oralis</i> , 5', 4.6kb / <i>S. pneumoniae</i> , 3'	16.2	29.9
7	ABC-type transport system	<i>S. pneumoniae</i>	4.5	38.0
15	Phage element	<i>S. pneumoniae</i>	10.1	36.6
12	Unknown	<i>S. pneumoniae</i>	4.7	29.2
13	Unknown	<i>S. parasanguinis</i>	1.7	32.2

¹The very high quality ST448 strain ECC_3510 genome was arbitrarily selected to identify patterns of clustering among the genes of difference in ECC strains. A cluster is defined as 2 or more contiguous genes.

²Refer to Supplementary Data 4 for full list of genes associated with each cluster.

³Based on highest BLAST result on nucleotide sequence.

^{a,b}Clusters that are not found on a single contig, but could be linked together by synteny analysis versus a closed reference genome.